

Macroscopic Friction Coefficient Measurements on Living Endothelial Cells

Alison C. Dunn · Toral D. Zaveri ·
Benjamin G. Keselowsky · W. Gregory Sawyer

Received: 14 December 2006 / Accepted: 30 April 2007 / Published online: 31 May 2007
© Springer Science+Business Media, LLC 2007

Abstract Arterial stent deployment by balloon or self-expandable structure introduces shear forces and radial forces that can damage or remove the endothelial cell layer. These factors can subsequently cause failure by restenosis or endothelial leaks. These conditions can be exacerbated by pulsatile blood flow and arterial asymmetry, which can cause migration or displacement. In mechanical or finite-element models which attempt to explain this motion, friction between the stent materials and endothelial cells is eclipsed by pressure, or assumptions that cells are moved along with the stent. During device deployment or migration, some relative motion between stent materials and endothelial cells occurs. This study aims to quantify friction between a polished glass pin and a single layer of arterial endothelial cells, and include observations of cell damage in an attempt to better understand the biological response to tribological stresses. Measured friction coefficient values were on the order of $\mu = 0.03\text{--}0.06$.

Keywords Biotribology · Stent · Cells

Introduction

Vascular tribological research often focuses on the materials and mechanics associated with arterial stents and

catheters [1]. Coronary artery stents are scaffold-like medical devices that are inserted into a damaged artery and opened in an effort to stabilize the vessel diameter, and blood flow. Biocompatible materials that have been used to create these scaffolds are the following: stainless steel, cobalt–chromium–nickel–molybdenum–iron alloys, tantalum, nitinol, polyethylene, polyurethane, and ePTFE coated nitinol to name a few [2]. Figure 1 illustrates an artery with a stent during expansion into contact with the endothelial cell layer (greatly exaggerated) that makes up the inner lining of a healthy artery. This research reports on the measurements of the friction forces between a smooth inert surface and a confluent layer of bovine aortic endothelial cells (BAEC). There are a number of biotribological interactions of importance in stent design, insertion, and fixation. We are unaware of any direct contact tribology experiments on endothelial cells. Nanotribology techniques such as atomic force microscopy (AFM) have been used to assess mechanical properties, but have not as yet identified friction coefficient values [3]. At the macroscale, synthetic arteries have been constructed to assess the forces necessary to prevent retrograde displacement; the predicted forces for typical geometries are in the range of 2.05 ± 0.02 N [4].

Preliminary theoretical efforts to quantify the forces necessary to displace a stent focused on control volume analysis of a specific area of an artery [5]. A variety of commercial stents were compared with these studies, with predicted displacement forces from 4.5–25 N [6]. The radial pressure stiffness, an additional mechanical parameter of a stent, was identified and compared to various methods of testing the stiffness of a cylindrical tube [7]. Fluid mechanics computations have also been used to predict these drag forces on stent-grafts, finding typical values in the range of 3.9–5.5 N [8].

A. C. Dunn · W. G. Sawyer (✉)
Department of Mechanical and Aerospace Engineering,
University of Florida, Gainesville, FL 32611, USA
e-mail: wgsawyer@ufl.edu

T. D. Zaveri · B. G. Keselowsky
J. Crayton Pruitt Family Department of Biomedical Engineering,
University of Florida, Gainesville, FL 32611, USA

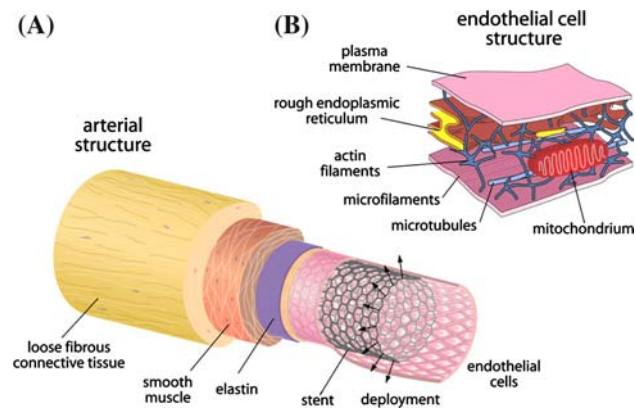


Fig. 1 (A) Schematic of a stent located inside of the arterial structure. (B) Schematic of the structure of an endothelial cell including the structural elements such as the actin filaments (blue), microfilaments (light blue), and microtubules (lining the bottom plasma membrane)

Finite element models [9, 10] based on fluid mechanics along with the mechanics of the stents themselves [11] allow more cohesive models of stent/artery behavior, including fixation, drag forces, and displacement. Experimental investigations of the non-linear stress-strain behavior of stent devices [12, 13] has increased the accuracy of these models as well. Displacement forces of these models are limited to less than 5 N. Frictional work on the endothelium during stent implantation runs up to 700 μ J (140 mN moving 5 mm, for example) [14]. Extensive finite-element modeling requires some frictional parameters, which thus far have been provided by large-scale drag or displacement forces. Holzapfel describes the following: “Although our contact approach is able to capture frictional behavior, we carried out the simulations without friction since reliable coefficients describing the frictional behavior between the intimal surface and the stent are not available yet” [15].

The substantial body of research on endothelial cell response to shear flow has improved the understanding of the biological reaction of the cellular structure under such steady shear stresses [16]. Mechanical properties such as elasticity have been shown to change with cells cultured under a fluid shear flow [17, 18]. Cells have been cultured directly on stent materials including titanium alloys, Nitinol, and stainless steel. Cell number was seen to be comparable to a control (plastic with collagen treatment) on TiN and TiO₂, with decreased cell number on Nitinol and stainless steel [19]. Unfavorable interactions with these materials may contribute to lower fixation and therefore increased migration of the stent device.

Though the endothelium of human arteries is designed to thrive under shear flows of blood, stents introduce contacting shear stresses during expansion, and possibly

during migration. The differences in friction between smooth muscle cells and endothelial cells in contact with stent materials are not yet known. The primary aim of this study is to hone a technique for applying very light contact shear stresses to a cultured cell layer, and to quantify friction results. The secondary aim is to observe any damage caused, and correlate it with the cellular response. It is hypothesized that if the friction between a smooth inert surface such as borosilicate glass and a single layer of BAECs can be measured, it will be on the order of other soft biological materials such as tissue or hydrogel materials ($\mu \sim 0.03\text{--}0.1$).

Materials and Methods

Bovine aortic endothelial cells (BAEC) were cultured in endothelial cell basal medium with growth supplements human endothelial growth factor (hEGF), hydrocortisone, fetal bovine serum (FBS) and GA-100 (Clonetics ECM-MV Bulletkit), purchased from Cambrex Bioscience Walkersville Inc. (Walkersville, MD). On attaining 100% confluency BAECs were subcultured using 0.25% Trypsin EDTA 1 \times (Cellgro Mediatech Inc, Herndon, VA) passaged at a 1:3 ratio. BAECs from passage 6 were seeded on 9 mm diameter wells created by removing the gaskets from chambered coverslips (Electron Microscopy Sciences, Washington, PA) and placing them onto tissue culture-treated polystyrene dish surfaces. To accommodate testing, tissue culture dishes were cut with a hot scalpel as shown in Fig. 2. Each well was seeded with 9×10^4 cells and incubated overnight for cells to reach the 100% confluency required for friction testing.

Friction tests were run in a pin-on-flat configuration in reciprocating sliding on the confluent cell layer cultured on tissue culture-treated polystyrene in the presence of 10% serum. Three tests locations in parallel were run in each culture well at a sliding speed of 300 μ m/s and an average applied load of 0.4 mN (Table 1). The experimental apparatus used to run these friction tests is a customized microtribometer (Fig. 2) [20]. It has been modified to achieve submerged sample capability, lower applied normal loads, and easier data acquisition and processing. The pin is a plano-convex glass lens with radius $R = 7.78$ mm. The capillary forces from the submerged cylindrical pin are zeroed manually after contact with the cell layer has been located. For each sliding cycle, the average normal force, F_n , and friction force, F_t , are calculated from the middle 30% of the sliding region, s . Force feedback is achieved by adjusting a vertical piezoelectric cell according to the difference between the desired average normal load and that which is measured. Before and after testing, cells are observed under a 10 \times objective in a Leica DMLM microscope

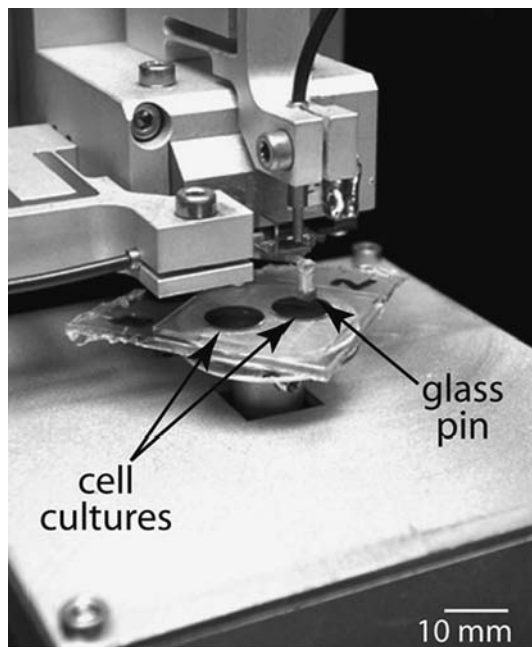


Fig. 2 A photograph of the experimental apparatus showing the glass pin above the cell culture wells, which is mounted on the reciprocating stage. The pin and flexure motion is measured by the displacement of optical sensors

using the DIC/Nomarski mode. Immediately after friction testing in order to preserve the actin cytoskeletal arrangement, the cells were washed with phosphate buffered saline (PBS) to remove the excess Trypan blue and permeabilized in 0.5% Triton-X in PBS for 10 min. After permeabilizing, the cells were fixed in 3.7% formaldehyde for 10 min and then left in blocking buffer (5% FBS in PBS with 0.01% Sodium azide) for 45 min [21, 22]. The cells were then stained for actin using rhodamine phalloidin (Molecular Probes, Inc., Eugene, OR) [23]. The fluorescence images were obtained using an Axiovert 2000M.

The experimental procedure of cell observation and friction tests is as follows:

- (1) Cell chambers are removed from incubator and the growth media is replaced. Cells are transported between laboratories.
- (2) Growth media in cell chambers is replaced with a dilution of 1:10 Trypan blue 0.4% solution and observed under a 10× objective to check for a single layer of viable confluent cells.
- (3) The chamber is secured with double-sided adhesive to a stub, which is mounted to the tribometer reciprocating stage.
- (4) The pin is lowered into contact with the cells and normal load is slowly applied (~0.05 mN/s).
- (5) Stage reciprocates; force and position data is collected continuously at 1 kHz.

- (6) The chamber is removed and transported back to the microscope, and Trypan blue replaced by growth media.
- (7) Cells are checked for viability under 10× objective, then fixed with formaldehyde, and transported back to the cell laboratory.
- (8) Cells are stained with actin stain and observed under 10× objective before disposal.

Friction and Wear Results

The normal loads applied on average for each test were in the range of 0.4–1.2 mN, which encompass multiple modes of cell interactions and wear results. Thus, rather than report an average friction coefficient from each test, the forces were plotted against each other: F_n vs. F_t (Fig. 3). This type of plot can illustrate changes in friction coefficient with changes in normal force, which on the fragile cell layer could produce a wide range of responses. We take the friction coefficient to be the slope of the line through these points, $F_t = \mu F_n + \mu F_0$, where F_0 is an unknown adhesion force, and F_t and F_n are the measurands from the experiments.

A representative phase contrast image of a confluent monolayer of BAEC cells prior to friction testing is shown in Fig. 4. Trypan blue exclusion was used to assess cell viability on live cultures and background levels of Trypan

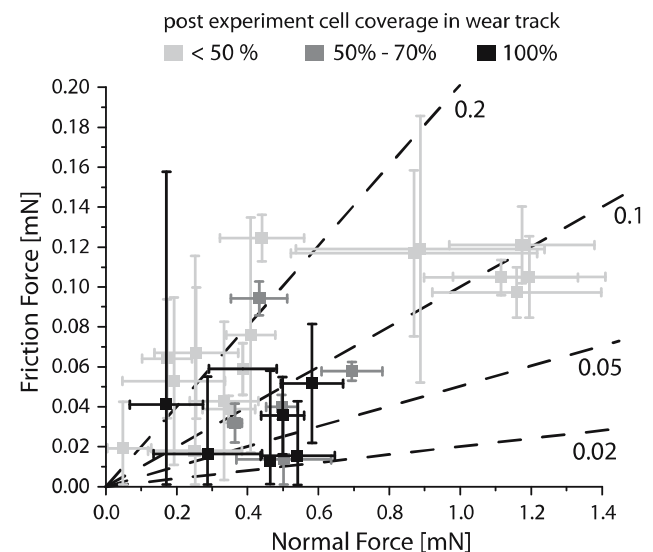


Fig. 3 Plot of frictional force as a function of normal force for each of three post-experiment conditions: less than 50% of cell coverage remaining, 50–70% of cell coverage remaining, and nearly 100% coverage remaining. Sample friction coefficients are the slopes indicated of $\mu = 0.02, 0.05, 0.1,$ and 0.2 . Higher friction coefficient values typically result when the cell layer has been removed by the relative sliding (lighter data points)

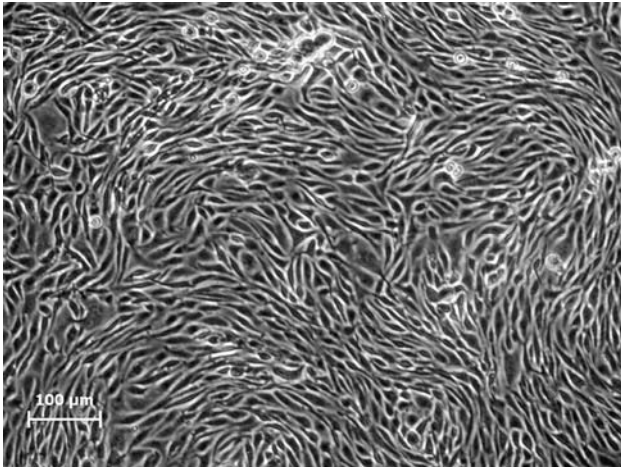
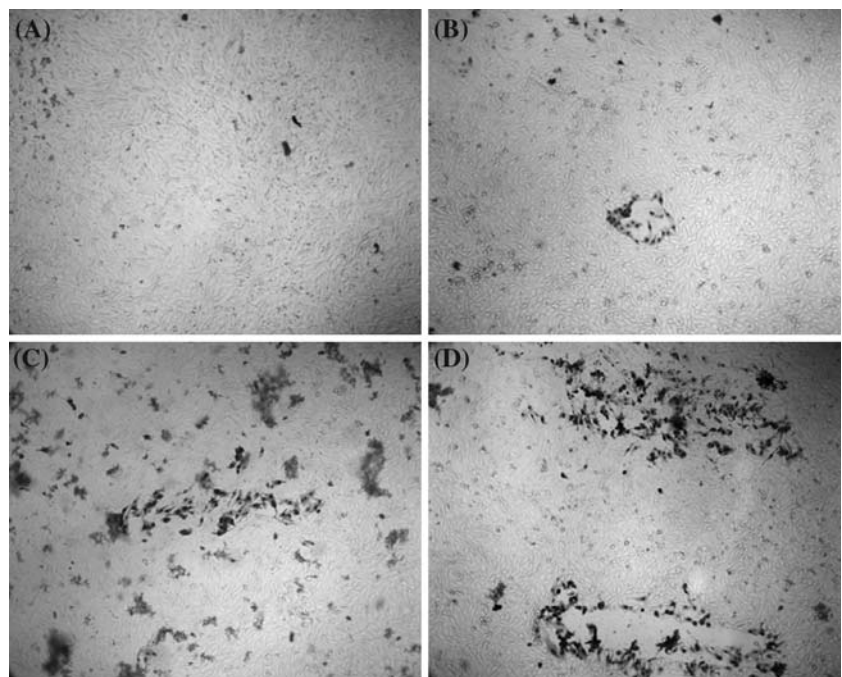


Fig. 4 Phase contrast image of initial BAEC cell seeding showing the random arrangement of the cells prior to friction tests. Scale bar in the lower left corner is 100 μm

blue staining were low (Fig. 5A). Touchdown forces of 5 mN or greater demonstrated cell death at the point of contact (Fig. 5B). Cell death due to shear stress was observed along the pin path under conditions where the endothelial cell monolayer was left intact (one sliding cycle, Fig. 5C) and when the pin broke through the monolayer (three sliding cycles or more, Fig. 5D). Immunofluorescence staining of actin cytoskeleton demonstrated formation of aligned stress fibers in parallel with the direction of force, in response to shear stress (Fig. 6), in agreement with previous findings for this cell type [24, 25].

Fig. 5 DIC images of the Trypan Blue (which shows up as black) stained cell layer at 10 \times magnification after 2 h of time lapse for the following tests: (A) control with no test, (B) a single touchdown at a higher load (5 mN), (C) sliding friction test with some cell death, but no cell removal, and (D) sliding friction tests with gross cell death and removal



Damage was categorized for each test according to the following conditions: black data points for those tests where no cells were removed, but some cell death occurred (100% cell coverage post-testing); gray data points for those tests in which some cells were removed, and there was some cell death (50–70% coverage post-testing); and light gray data points for those tests in which a majority of the cells were removed (<50% coverage post-testing).

Based on those categories, it would appear that normal loads applied to the BAEC layer above 0.7 mN produce frictional detachment forces high enough to overcome the adhesion forces between the cells and the substrate and between adjacent cells. Shear stresses are on the order of 0–2 kPa. Applied forces below 0.7 mN allow some cells to remain on the surface (applied stress order 3 kPa).

A least squares regression line through the points where cells remained confluent for all cycles of the test indicates a friction coefficient of $\mu = 0.03 \pm 0.02$, which is similar to other lubricated and soft biological materials such as hydrogels [20]. A slope through the other points would indicate a slope of $\mu = 0.06 \pm 0.01$, which corresponds to the expected response of sliding between glass and cell growth substrate of tissue culture polystyrene.

Discussion

Many factors contribute to the uncertainty of these measurements, including voltage acquisition resolution and cell growth parameters (age of media, seeding density, growth

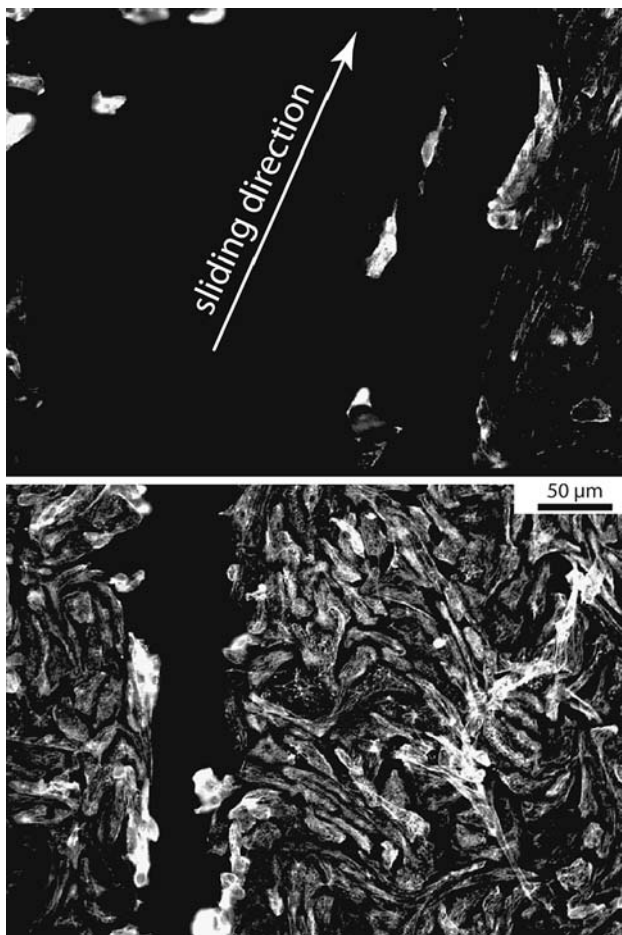


Fig. 6 Immunofluorescence staining of actin stress fibers at the edge region of the sliding tests where some cells were detached. Bright regions indicate bundling of structural actin fibers and alignment along the sliding direction within the cells (actin fibers have been stained and show up white). Solid black regions are void of cells

Table 1 Experimental testing conditions of cultured cells

Average normal load	F_n	0.4 mN
Wear path length	s	500 μm
Sliding speed	V	300 $\mu\text{m/s}$
Relative humidity		46–51%
Temperature		28 °C air, 28 °C liquid
Sampling rate		1000 Hz

time, etc.). While the contact pressures were fairly high for cells (up to 3 kPa) due to the infinitely hard substrate and pin (tissue culture-treated polystyrene and glass) as compared to the cell layer, this system may serve as an appropriate model for stent deployment in a location of atherosclerotic plaque. Given more compliant cell culture substrates, the contact pressure could be further decreased in the cell layer to reflect healthy vasculature. Pressures on the order of 5 kPa are required to cause significant damage

to a cell layer. Blood pressure can rise to damaging levels, reaching 16 kPa in severely hypertensive patients [26]. Cell death or cell removal from the endothelium of an artery due to stresses of deployment could contribute to stent migration when put in the context of pulsatile blood pressures and the associated changes in momentum of the blood flow.

The vascular buildup that often necessitates stenting, such as diseased media, plaque, and calcification, is also a relevant contact surface for flow maintenance devices. The stiffnesses and mechanics of those materials may provide a vastly different tribology. Here the tribology of a well-described endothelial system against a polished glass pin is described during sliding. The sensitivity of the cells to sliding motions and repeated loading was evident using the staining techniques. It is interesting to note how quickly the actin filament aligned during single passes of traction; this is shown in Fig. 6. Mechanics of the cell layer were not investigated. The pressures described earlier are computed based on the width of the wear scar that was observed from staining. It is important to note that upon contact with physiological fluids, proteins rapidly adsorb onto material surfaces [27–29]. In fact, material surface properties affect composition and functional activity of adsorbed proteins, modulating cellular adhesive responses [21, 30–31]. Friction tests were carried out in 10% serum and the glass pin used in this study is expected to be coated with serum proteins (e.g., vitronectin, albumin, and fibronectin). While protein adsorption would be expected to differ if carried out in the presence of whole blood, standard culturing conditions were used to avoid complications associated with use of whole blood/plasma, such as clotting and opaqueness. Due to the novelty of this type of testing, it is unclear, how different adsorbed proteins would affect contacting shear stresses on cell layers and warrants further investigation.

The inclusion of living biological materials in long duration tribological testing requires a number of future experimental modifications. The results reported here were collected in a tribometer that was not designed to continue providing nourishment or optimum growth conditions for the cells. Thus, experiments were concluded after a few sliding cycles (none exceeding 5 complete reciprocations). Future developments would be to reduce contact pressures to accommodate more relevant contact mechanics situations, include a light CO_2 gas partial pressure for continued cell viability over long testing times, and provide regulated temperature for un-interrupted culture during testing.

Closure

Micro-friction tests were run on BAEC layer in a customized micro-tribometer under low loads ($\bar{F}_n = 0.4$ mN),

and friction coefficient observed from $\mu = 0.03$ (no cells removed) to $\mu = 0.06$ (many cells removed). The pressures that exist in severely hypertensive patients are far higher than the shear and normal stresses used to cause significant cell damage, so stent migration could be a result of damaged cells due to pressure fluctuations of the pulsatile flow.

Acknowledgements The authors would like to acknowledge very helpful conversations regarding testing procedures and cell culturing with Prof. Roger Tran-Son-Tay, Prof. Malisa Sarntinoranont, and Jessica Cobb at the University of Florida.

References

- Ho, S.P., Nakabayashi, N., Iwasaki, Y., Boland, T., Laberge, M.: Frictional properties of Poly(Mpc-Co-Bma) phospholipid polymer for catheter applications. *Biomaterials* **24**(28), 5121–5129 (2003)
- Lim, I.: Biocompatibility of stent materials. MIT Undergrad. Res. J. **11**(Fall 2004), 33–37 (2004)
- Costa, K.D., Sim, A.J., Yin, F.C.P.: Non-hertzian approach to analyzing mechanical properties of endothelial cells probed by atomic force microscopy. *J. Biomech. Eng. Trans. Asme* **128**(2), 176–184 (2006)
- Volodos, S.M., Sayers, R.D., Gostelow, J.P., Bell, P.R.F.: An investigation into the cause of distal endoleaks: role of displacement force on the distal end of a stent-graft. *J. Endovas. Ther* **12**(1), 115–120 (2005)
- Liffman, K., Sutalo, I.D., Lawrence-Brown, M.M.D., Semmens, J.B., Aldham, B.: Movement and dislocation of modular stent-grafts due to pulsatile flow and the pressure difference between the stent-graft and the aneurysm sac. *J. Endovas. Ther* **13**(1), 51–61 (2006)
- Resch, T., Malina, M., Lindblad, B., Malina, J., Brunkwall, J., Ivancev, K.: The impact of stent design on proximal stentgraft fixation in the abdominal aorta: an experimental study. *Eur. J. Vasc. Endovasc. Surg.* **20**(2), 190–195 (2000)
- Jedwab, M.R., Clerc, C.O.: A study of the geometrical and mechanical-properties of a self-expanding metallic stent theory and experiment. *J. Appl. Biomat.* **4**(1), 77–85 (1993)
- Morris, L., Delassus, P., Walsh, M., Mcgloughlin, T.: A mathematical model to predict the in vivo pulsatile drag forces acting on bifurcated stent grafts used in endovascular treatment of abdominal aortic aneurysms (Aaa). *J. Biomech* **37**(7), 1087–1095 (2004)
- Li, Z., Kleinstreuer, C.: Analysis of biomechanical factors affecting stent-graft migration in an abdominal aortic aneurysm model. *J. Biomech* **39**(12), 2264–2273 (2006)
- Li, Z., Kleinstreuer, C., Farber, M.: Computational analysis of biomechanical contributors to endovascular graft failure. *Biomech. Model Mechanobiol.* **4**(4), 221–234 (2005)
- Walke, W., Paszenda, Z., Filipiak, J.: Experimental and numerical biomechanical analysis of vascular stent. *J. Mater. Process. Technol.* **164**, 1263–1268 (2005)
- Wang, R., Ravi-Chandar, K.: Mechanical response of a metallic aortic stent - Part I: Pressure-diameter relationship. *J. Appl. Mech. Trans. Asme* **71**(5), 697–705 (2004)
- Wang, R., Ravi-Chandar, K.: Mechanical response of a metallic aortic stent - Part II: A beam-on-elastic foundation model. *J. Appl. Mech. Trans. Asme* **71**(5), 706–712 (2004)
- Laroche, D., Delorme, S., Anderson, T., Diraddo, R.: Computer prediction of friction in balloon angioplasty and stent implantation. *Biomed. Simul., Proc.* **4072**, 1–8 (2006)
- Holzappel, G., Stadler, M., Gasser, T.C.: Changes in the mechanical environment of stenotic arteries during interaction with stents: computational assessment of parametric stent designs. *J. Biomech. Eng. Trans. Asme* **127**(1), 166–180 (2005)
- Fisher, A.B., Chien, S., Barakat, A.I., Nerem, R.M.: Endothelial cellular response to altered shear stress. *Am. J. Physiol. Lung Cell. Mol. Physiol.* **281**(3), L529–L533 (2001)
- Sato, H., Katano, M., Takigawa, T., Masuda, T.: Estimation for the elasticity of vascular endothelial cells on the basis of atomic force microscopy and Young's modulus of gelatin gels. *Polym. Bull.* **47**(3–4), 375–381 (2001)
- Sato, M., Nagayama, K., Kataoka, N., Sasaki, M., Hane, K.: Local mechanical properties measured by atomic force microscopy for cultured bovine endothelial cells exposed to shear stress. *J. Biomech.* **33**(1), 127–135 (2000)
- Yeh, H.I., Lu, S.K., Tian, T.Y., Hong, R.C., Lee, W.H., Tsai, C.H.: Comparison of endothelial cells grown on different stent materials. *J. Biomed. Mater. Res. A* **76A**(4), 835–841 (2006)
- Rennie, A.C., Dickrell, P.L., Sawyer, W.G.: Friction coefficient of soft contact lenses: measurements and modeling. *Tribol. Lett.* **18**(4), 499–504 (2005)
- Keselowsky, B.G., Collard, D.M., Garcia, A.J.: Surface chemistry modulates focal adhesion composition and signaling through changes in integrin binding. *Biomaterials* **25**(28), 5947–5954 (2004)
- Keselowsky, B.G., Garcia, A.J.: Quantitative methods for analysis of integrin binding and focal adhesion formation on biomaterial surfaces. *Biomaterials* **26**(4), 413–418 (2005)
- Keselowsky, B.G., Wang, L., Schwartz, Z., Garcia, A.J., Boyan, B.D.: Integrin alpha(5) controls osteoblastic proliferation and differentiation responses to titanium substrates presenting different roughness characteristics in a roughness independent manner. *J. Biomed. Mater. Res. A* **80A**(3), 700–710 (2007)
- Butcher, J.T., Tressel, S., Johnson, T., Turner, D., Sorescu, G., Jo, H., Nerem, R.M.: Transcriptional profiles of valvular and vascular endothelial cells reveal phenotypic differences - influence of shear stress. *Arterioscler. Thromb. Vasc. Biol.* **26**(1), 69–77 (2006)
- Galbraith, C.G., Skalak, R., Chien, S.: Shear stress induces spatial reorganization of the endothelial cell cytoskeleton. *Cell Motil. Cytoskeleton* **40**(4), 317–330 (1998)
- Mohan, I.V., Harris, P.L., Van Marrewijk, C.J., Laheij, R.J., How, T.V.: Factors and forces influencing stent-graft migration after endovascular aortic aneurysm repair. *J. Endovasc. Ther.* **9**, 748–755 (2002)
- Ratner B.D., Bryant S.J.: Biomaterials: where we have been and where we are going. *Annu. Rev. Biomed. Eng.* **6**, 41–75 (2004)
- Brash J.L.: Protein adsorption at the solid-solution interface in relation to blood-material interactions. In: Horbett T.A., Brash J.L. (eds) *Proteins at Interfaces*, pp. 490–506. American Chemical Society, Washington, DC (1987)
- Andrade, J.D., Hlady, V.V.: Protein adsorption and materials biocompatibility: a tutorial review and suggested hypotheses. *Adv. Polym. Sci.* **79**, 1–63 (1986)
- Keselowsky, B.G., Collard, D.M., Garcia, A.J.: Integrin binding specificity regulates biomaterial surface chemistry effects on cell differentiation. *Proc. Natl. Acad. Sci. U.S.A* **102**(17), 5953–5957 (2005)
- Keselowsky, B.G., Collard, D.M., Garcia, A.J.: Surface chemistry modulates fibronectin conformation and directs integrin binding and specificity to control cell adhesion. *J. Biomed. Mater. Res. A* **66A**(2), 247–259 (2003)